Journal of Chromatography, 400 (1987) 47–63
Elsevier Science Publishers B.V., Amsterdam — Printed in The Netherlands

CHROMSYMP. 1204

TAIL-PRODUCING SLOW ADSORPTION–DESORPTION PROCESS IN LIQUID–SOLID CHROMATOGRAPHY

TOSHIKAZU OHKUMA and SHOJI HARA*
Tokyo College of Pharmacy, Horinouchi, Hachioji, Tokyo 192-03 (Japan)

SUMMARY

The tailing peak shape observed in liquid–solid chromatography is analysed on the basis of the assumption that peak tailing at high solute dilution is a kinetic effect of slow adsorption–desorption processes. Gaussian functions are fitted to the leading profiles of experimental peaks, and the portions of the peaks deviating from the Gaussian functions are separated as apparent tail portions. The fractional area of the apparent tail portion decreases and its relative length with reference to the elution time increases with increasing mobile phase flow-rate, indicating that this portion of the peak is strongly influenced by the kinetic effect of slow processes. By adding a small amount of water to the mobile phase the fractional tail area is diminished and an almost Gaussian profile is obtained. The role of water in reduction of the tail area is to retard the adsorption of solute molecules in the slow process.

INTRODUCTION

In liquid–solid chromatography (LSC) with polar adsorbents the main problem regarding separation efficiency is the tendency of highly polar solutes to give rise to "peak tailing". The peak asymmetry in LSC is attributed in part to the non-linearity of the relevant isotherm and solute overloading. However, the peak tailing phenomenon persists even at high solute dilution and it has the character of kinetic effects, *i.e.*, the appearance and degree of peak tailing depend on elution time, as will be discussed below. For such behaviour of polar solutes to occur in LSC, it may be necessary for a distinctively slow adsorption–desorption process to take place in LSC, together with rapid exchanges.

The effects of such slow kinetics on chromatographic peak shape (kinetic tailing) were first discussed by Giddings[1,2] on the basis of stochastic theory. Accordingly, if the exchange of solute molecules between the mobile and stationary phase is sufficiently rapid, as is usually assumed, the injection of a very minute volume of an infinitely dilute sample yields a eluite zone of Gaussian form almost instantaneously. However, if there exist in the stationary phase some special sites on which solute molecules are slowly adsorbed and desorbed, a significant portion of the injected solute molecules are eluted without being captured by these sites, and those captured at least once by the sites take part in the formation of an additional eluite zone

0021-9673/87/$03.50

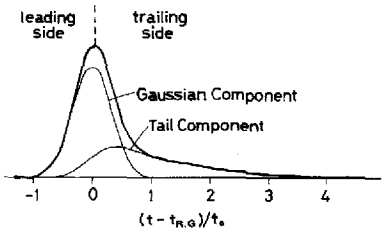

Fig. 1. Simulated elution chromatogram, representing the tail-producing effect of a slow adsorption–desorption process with finite first-order adsorption and desorption rate constants.

("tail") after the Gaussian zone, as shown in Fig. 1. The area of the tail relative to that of the whole peak depends on the adsorption rate constant on the "tail-producing sites" and the Gaussian zone elution time, while the length of the tail relative to the Gaussian zone elution time depends on the desorption rate constant on the sites and the elution time.

In previous papers[3,4] we showed that at high solute dilution the LSC peak widths of polar solutes are reduced by the addition of a small amount of highly polar solvent, such as methanol or water, to the mobile phase. Most of these reductions in peak width were accompanied by decreases in the peak asymmetry, measured at 10% of the peak height. From the above discussion, such a change in peak shape may be regarded as either or both of the following two possible effects of additive polar solvents, acting on the slow adsorption–desorption process in LSC: (a) reduction in peak-tail length by accelerating desorption on tail-producing sites and (b) reduction in peak-tail area by retarding adsorption on tail-producing sites.

In order to differentiate between these effects, we have devised a method for evaluating the area and length of the tail. In this method, a simplified equation, developed by Chesler and Cram[5], for representing peak shape is used. A Gaussian function is fitted to the leading profile of an experimental peak, and the portion deviating from the Gaussian is described by an empirically devised function as an "apparent tail portion".

The aim of this paper is a qualitative analysis of the peak-tailing phenomenon in LSC by the above method.

EXPERIMENTAL

Chemicals

The deoxynucleoside derivatives chosen as sample solutes were prepared in our laboratory from deoxynucleosides according to a literature procedure[6]. The reagents used for sample preparation, other sample solutes and solvents were purchased from Wako (Osaka, Japan).

Chromatographic experiments

All chromatographic experiments were carried out on a Model 5021 chromatograph (Varian, Palo Alto, CA, U.S.A.). The column was 250 mm × 4 mm I.D., packed with LiChrosorb Si-60 with a particle size of 5 μm (Merck, Darmstadt, F.R.G.).

The column was thermostated at 40°C by heating jacket. Mobile-phase solvent mixtures were introduced into the column by a reciprocal pump, equipped with a pulse damper. Each sample solute was dissolved in the mobile phase examined, at a concentration about $1 \cdot 10^{-5}$ M, and about 1 μl of this solution was injected into the column by a Valco sampling valve. An SPD-1 UV detector (Shimadzu, Kyoto, Japan) was used, having a cell volume of 6.4 μl and a path length of 8 mm. The wavelength used was 280 nm. The stainless-steel tubing connecting the injector, column and detector with each other was of 0.1 mm I.D.

DATA HANDLING AND CALCULATIONS

Chromatographic data acquisition

Detector responses were introduced into the data processor (Model 8000A; System Instruments, Tokyo, Japan) during each chromatographic run and recorded to obtain a digital chromatogram, which was then stored on an 8-in. magnetic disk. On the data processor, the chromatogram was converted at the next step into discrete point data, consisting, depending on the relative length of the peak tail, of 100–200

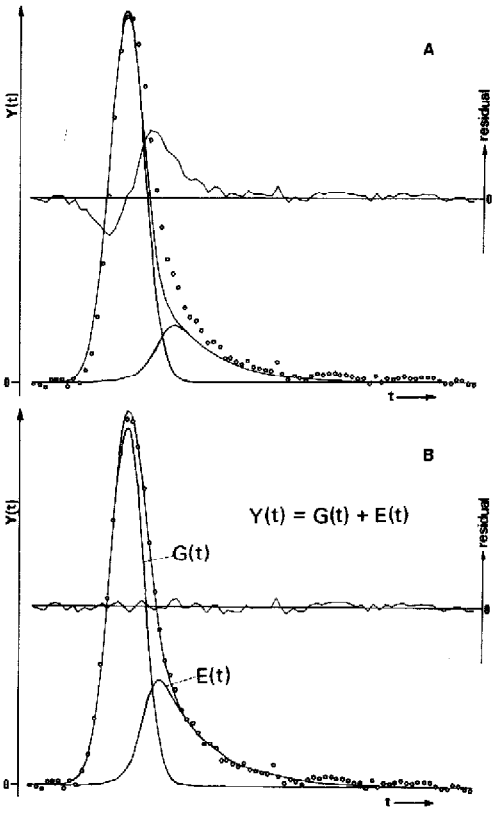

Fig. 2. Fitting of the Chesler–Cram equation to a discrete point chromatogram (○), and plots of residuals between data points and total function values: (A) initial estimate; (B) best fit.

points picked up at constant intervals, so that about ten points were taken from the leading side of the peak. The discrete point data were transferred from the data processor to the 16-bit microcomputer (PC 9801; NEC, Tokyo, Japan), on which the peak shape was examined. All programs for treating the discrete point data were written in BASIC.

The baseline level of the transferred discrete point chromatogram was corrected for long-term baseline drifts. Two sets of succesive data points (about ten points) were chosen from the regions of time preceding and succeeding the objective peak. Each set of points was arithmetically averaged to determine the zero level of the mid-point time of the set of points. The zero levels for the intervening (peak) region were determined by a straight line, linking the two average values of the two end regions. The corrected data points between the mid-point times of the two end regions were used for curve fitting (see Fig. 2).

Curve-fitting procedure

Most of the curve-fitting procedure was carried out in accordance with a paper by Chesler and Cram[5]. Certain points were modified, especially those for the initial estimate determinations.

The Chesler–Cram equation is

$$Y(t) = G(t) + E(t) \tag{1}$$

Where $Y(t)$ is the vertical axis amplitude on the chromatogram at time t and $G(t)$ is the Gaussian function:

$$G(t) = P_1 \exp\left[-(t - P_4)^2/2P_5\right] \tag{2}$$

$E(t)$ is an exponentially decayed hyperbolic tangent (EH) function which has been empirically devised and is used to represent tail distributions in this study:

$$\begin{aligned} E(t) = {} & 0.5\, P_1 P_6 \{\tanh[P_2\,(t - P_3)] + 1\} \\ & \{\exp[-0.5\, P_7(|t - P_8| + t - P_8)]\} \end{aligned} \tag{3}$$

$P_1 - P_8$ are parameters of this non-linear equation. Their values in the initial step were set in the following way for each corrected discrete point chromatogram. P_1 and P_4 were given as the amplitude and time of the peak maximum, respectively. P_2 and P_3 were given as functions of the initial P_5.

$$P_2 = 1/\sqrt{P_5}; \qquad P_3 = P_4 + 2\sqrt{P_5} \tag{4}$$

P_5 was given as the square of the difference between the initial P_4 and time of the point nearest to the amplitude level of $0.607P_1$ in the leading side of the peak. P_6 and P_7 were given as follows:

$$P_6 = P'_6/[P_1 \exp(-8\sqrt{P_5}\, P'_7 / P'_6)]; \qquad P_7 = P'_7 / P'_6 \tag{5}$$

where P'_6 and P'_7 are the absolute values of the mean amplitude and slope, respectively, at time $P_4 + 4\sqrt{P_5}$, determined by averaging six points near this time. P_8 was given as $P_4 - 4\sqrt{P_5}$.

These parameter values were used in the above equation (Fig. 2A), and the residuals between corrected data points and corresponding Y values calculated from the equation were used, in a feedback mode, to alter iteratively the parameter values so that the sum of the squared residuals would eventually diminish. The least-squares method used for this parameter alteration was according to Roberts *et al.*[7].

The iterative process consisted of two stages. In the first stage, certain accelerating techniques and constraints were applied in calculating altered parameter values for the rapid and stable convergence of residual diminution. The forcing factor ($=2$) was applied to the diagonal terms of the matrix for the set of normal equations involved in the least-squares method, as in ref. 7. In the course of the first four iterative steps, the following two constraints were implemented. If an altered value exceeded the 1.1-fold value of the one-step-former value, the parameter value was set to the 1.1-fold value. The initial value of P_8 was maintained through the four steps. When the difference in the sum of squared residuals between two successive steps was less than one tenth the sum of the first of the two steps, this stage was no longer continued.

In the second stage, iteration proceeded without acceleration and constraints until the difference in the squared residual sum between the successive steps became less than one-thousandth the former sum value. The iteration was then terminated, and the parameter values for the best-fitted curve were determined (Fig. 2B).

Area calculation

Areas under the fitted curves were calculated numerically, as these functions are not directly integrated in closed forms. The Simpson quadratic approximation was used to obtain the numerical solutions.

The ranges of time over which the quadratic approximations were applied were determined as follows. The range for the fitted Gaussian function was that covered, centering around the Gaussian mid-point time, by a radius of six times the determined $\sqrt{P_5}$ value. The amplitude for the limits of both sides is the $1.5 \cdot 10^{-8}$-fold value of P_1. The range for the fitted EH function was determined so that it would have the same limit amplitude value as that of the Gaussian function.

The approximated value for area was repeatedly calculated, while the unit time period for which single quadratic functions were fitted to portions of curves was reduced by gradually bisecting the entire range. When the difference between the area estimates of two successive steps became less than $5 \cdot 10^{-7}$ times the former estimate of the two, calculation was terminated and the area was determined.

The reliability of the present area approximation was checked indirectly by calculating a higher order moment which always requires a better accuracy than that for the zeroth moment (area). The theoretical value of the "excess" for a Gaussian distribution is exactly zero, and the calculated absolute value was reduced by the present approximation to less than $1 \cdot 10^{-5}$.

By use of experimental chromatograms with a high signal-to-noise ratio ($< 1\%$ for the relative standard deviation of baseline noise with reference to the peak height),

the standard deviation for the residuals between experimental data and corresponding fitted-curve values was reduced to less than 1.5% with reference to the peak height. As a result, the fractional areas of tails relative to total peak areas were determined with standard deviations less than 5% with reference to the average values of the fractional areas.

THEORETICAL

Basic assumption

As shown in Figs. 3–6, LSC gives almost symmetric Gaussian peaks for certain solutes and tailing peaks for others at high solute dilution. From this fact, it may be assumed that there exists some process in LSC to convert peak shapes from original Gaussian forms to tailing forms. As described above, this conversion may be caused by the presence of distinctively slow adsorption–desorption processes which produce tails at the expense of original Gaussian zones. In this respect, the tails represent the distributions of solute molecules captured at least once by tail-producing sites (captured solute molecules). Our peak-shape analysis was developed on the assumption that the apparent tail portion, which is separated in a subtractive manner by fitting a Gaussian function to the leading profile of the peak, represents the distribution of the captured solute molecules.

However, the actual tail distribution formed by captured solute molecules may be correctly separated by the present procedure, provided that the captured and uncaptured molecules are predominant in the formation of the trailing and leading edges of peaks, respectively. Many tailing peaks obtained in the LSC system at high solute dilution have nearly symmetric Gaussian-like top shapes, possibly attributable to the predominance of uncaptured molecules in the leading side. The distribution of the captured and uncaptured molecules can be fairly separated by the present procedure, as the top of this distribution may actually be located in the neighbourhood of the peak maximum and hence be reliably estimated by the procedure.

As the relative height of the captured molecule distribution increases, these molecules should determine for the most part the profiles of both sides of the peaks. The Gaussian shape of the uncaptured molecule distribution may then become indistinctive in the peak profile, which may be wholly asymmetric. Peak shapes of this type were observed for polar solutes eluted in non- or less-hydric LSC mobile phases (Fig. 4A). The leading side profiles of these peaks greatly differed from Gaussian forms. By the Chesler–Cram procedure, the actual uncaptured molecule distributions may not necessarily be found from these peaks, because the empirical EH function is used to describe the tails. Our peak shape analysis is therefore limited to peaks of the former type, having nearly Gaussian tops and relatively small tail heights, and the basic assumption will be tested by this analysis.

Fractional tail area

In the above limitation, the ratio of the apparent tail area to the total peak area (fractional tail area) obtained for a solute sample eluted in LSC is considered to be equal to the overall molar fraction of solute molecules that have participated in some slow adsorption–desorption process in the LSC column during solute zone elution. The molar fraction of captured molecules is an increasing function of the

zone elution time and the adsorption rate constant of the slow process. It decreases with increasing flow-rate of the mobile phase, as the zone elution time decreases with increasing flow-rate. If the apparent tails actually reflect captured solute molecules, area fractions must decrease with increasing flow-rate, and peak shapes will approach Gaussian forms.

Relative tail length

The degree of extension of the peak trailing edge, observed as the length of the apparent tail, is regarded as resulting from the slow desorption of captured solute molecules on the tail-producing sites. The desorption rate constant of the slow process determines the degree of dispersion of captured solute molecules in chromatographic development. When the migration of uncaptured molecules is so fast that it cannot be followed by the desorption of captured molecules, the captured molecule distribution may have a significant length in the trailing side of the peak. The ratio of this length to the Gaussian zone elution time becomes larger when zone migration is faster. Hence the basic assumption will be tested in this regard by examining the ratio of apparent tail length to elution time of the Gaussian component (relative tail length).

The length of the apparent tail portion is evaluated from its relative height and area because of relatively large errors in describing the portions of the peaks near the baseline with reference to those for the portions near the tops of apparent tails. If a captured molecule distribution is more dispersed with its fractional area remaining constant, its height will decrease. A decrease in tail height corresponds to an increase in tail length. Tail length can be evaluated comparatively by assuming that the shape of the actual tail function is constant and tail height is inversely proportional to tail length. The standard deviation for tail dispersion in time scale (σ_T) is thus expressed simply as

$$\sigma_T = c_T \, a_T / h_T \tag{6}$$

where a_T and h_T are the absolute values of tail area and height, respectively; c_T is constant but is not mathematically calculable here. The corresponding expression for the standard deviation of the Gaussian portion (σ_G) is

$$\sigma_G = c_G \, a_G / h_G \tag{7}$$

where c_G is constant and a_G and h_G are the corresponding area and height of the Gaussian component.

Combining eqns. 6 and 7, we obtain

$$\sigma_T = \frac{c_T \, a_T \, h_G}{c_G \, a_G \, h_T} \cdot \sigma_G \tag{8}$$

Here, the values of σ_G and ratios a_T/a_G and h_G/h_T can be precisely determined from the present curve fitting, but the ratio c_T/c_G is unknown. Because c_T/c_G is constant, we define a new quantity (σ'_T) to measure comparatively the length of apparent tail portion:

$$\sigma'_T = \frac{c_G}{c_T} \cdot \sigma_T = \frac{a_T h_G}{a_G h_T} \cdot \sigma_G \tag{9}$$

Accordingly, relative tail length is defined as $\sigma'_T/t_{R,G}$, where $t_{R,G}$ is the elution time for the top of the Gaussian portion (Gaussian retention time). In other words, eqn. 9 evaluates the degree of tail dispersion from the ratio of the reduced tail height, h_T/a_T, to the standardized Gaussian height, $h_G\sigma_G/a_G$, which corresponds to the height when the Gaussian portion is transformed so as to have unit area and width. Using this equation we can compare the tail lengths of peaks differing in fractional tail area and Gaussian width. It should be noted, however, that h_T is not completely independent of σ_G, although it is required to remain unchanged with varying σ_G. The Gaussian width, σ_G, is considered to be a cumulative effect of all band-broadening phenomena involved in LSC development, except the tail-producing process. The band-broadening process that determines σ_G should also influence the apparent tail distribution, especially in its leading part. When σ_G increases, the slope of the tail leading edge decreases and hence the tail height decreases. However, the effect of changes in σ_G on the tail height should be small relative to that on Gaussian height within a range of similar σ_G values, and it is neglected in the present analysis.

Extra-column effects

The basic assumption in the present analysis does not take into account the effects of the hydrodynamics of eluent flow outside the column on peak shape. However, it is necessary to distinguish these effects for characterizing the tail-producing process inside the column.

Extra-column asymmetric broadening effects observed on chromatograms can be caused by eluent flow pathways between the sample injection loop and the detector flow cell and/or by an electronic device which detects and records sample elution[8]. The peak-tailing phenomenon in the extra-column flow pathway may be modelled as the hydrodynamic effect of an expanded eluent chamber placed in the course of eluent flow pathway, which is not rapidly swept by the eluent flow because of its expanded diameter. The slow response effects of electronic devices in the detecting and recording system may be considered to be similar to those of the eluent chamber.

These extra-column effects can be conveniently described by means of the exponentially modified Gaussian model[9], in which peak asymmetries are related to the slow release of solute molecules from the hypothetical eluent chamber. Accordingly, as the flow-rate increases, the peak asymmetry should increase and the elution time should decrease to an extent less than that expected from the flow-rate change in the presence of sources of extra-column effects.

In Chesler–Cram curve fitting, the extra-column effect may possibly be observed as larger and longer apparent tails and/or poorer fits in the leading side of peaks at a higher flow-rate. When Chesler–Cram curves are excellently fitted to the leading side of a peak obtained at the higher flow-rate, the extra-column peak shape effect may be discussed on the basis of changes in apparent tail distribution. The magnitude of the extra-column effect convoluted in apparent tails will be evaluated by using the solute-non-specificity of this effect, *i.e.*, by examining less polar solutes which incur tail producing to a lesser extent (less-tailing solutes).

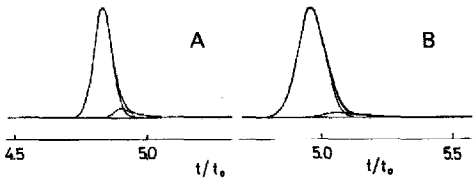

Fig. 3. Best fits of Chesler–Cram curves to experimental peaks of *n*-butyl phthalate, chromatographed on a silica gel column with *n*-hexane–ethyl acetate (98:2, v/v) at a flow-rate of (A) 1 ml/min and (B) 4 ml/min.

RESULTS AND DISCUSSION

Less-tailing solutes

Fig. 3 shows the best fits to peaks of *n*-butyl phthalate, eluted with *n*-hexane–ethyl acetate (98:2, v/v) at different flow-rates in the LSC system. The fitted Gaussian, apparent tail and total distribution for each peak are simultaneously plotted on the same coordinate system. The horizontal coordinates represent the time from injection relative to the hold-up time (t_0), corresponding to the column void volume. The column void volume was measured by eluting an *n*-hexane sample with the same mobile phase at a flow-rate of 1 ml/min, and the hold-up time at 4 ml/min was calculated from this measurement considering the expected error in measuring t_0 at this flow-rate caused by the extra-column effects. The elution time of this solute is longer at a higher flow-rate than expected from that at a lower flow-rate, suggesting the presence of an extra-column tailing source.

The leading and upper parts of both peaks fitted well to Gaussian forms, and departures from the Gaussian functions in the trailing side were estimated as small apparent tail areas. This fact permits us to discuss the effects of intra- and extra-column processes, using these apparent tail components, and to analyse these components according to the above principles.

The fractional tail areas, relative tail lengths and Gaussian widths of these peaks are shown in Table I. The relative tail length increases with an increase in flow-rate from 1 to 4 ml/min. This tail behaviour agrees with both of those expected independently on the assumptions of intra- and extra-column slow processes. However, these two processes should have counteracting effects on fractional tail areas. A 38% decrease in tail area is actually observed with a flow-rate increase, indicating that the influence of the intra-column process predominates in the change in tail distribution. Apart from the above-mentioned retention change, the extra-column effect on peak shape may be considered to be relatively small over the flow-rate range studied.

TABLE I

PEAK-SHAPE DATA FOR *n*-BUTYL PHTHALATE, CHROMATOGRAPHED ON A SILICA GEL COLUMN WITH *n*-HEXANE–ETHYL ACETATE (98:2, v/v)

Flow-rate (ml/min)	$a_T/(a_G + a_T)$	h_T/h_G	$10^3\sigma'_T/t_{R,G}$	$10^3\sigma_G/t_{R,G}$
1.0	0.090	0.083	8.4	7.1
4.0	0.056	0.047	12.0	9.5

It should be noted that when there are large voids in the column (as produced by cracking of column bed) the peak shape is analogous to that of slow adsorption–desorption kinetics if the voids act as diffusion chambers[8]. Including this void effect, extra-column band-broadening effects generally have a hydrodynamic character and depend on the solute diffusivity in the mobile phase, which is a function of mobile-phase composition and solute molar volume[10]. As long as comparisons are made among solutes that do not differ greatly, in molecular size and LSC retentivity and a series of hexane-based mobile phases are used, differences in diffusivity in an intra-column large void space or extra-column flow pathways should not give rise to any significant peak-shape differences. The magnitude of these effects can be considered to remain constant within such comparisons at a constant flow-rate.

Based on the above discussion, we can evaluate the effects of an intra-column process on the peak shape of a tailing solute. Whether or not a large void process takes part in the formation of the tails of less tailing solutes, the whole effect of intra- and extra-column processes on the peak shape may be relatively small for such solutes. For this reason, these peaks can be used as standards at the respective flow-rates. That is, if the apparent tail for a solute is larger than that of a less-tailing solute, it may be regarded as being produced mostly by an intra-column microscopic (adsorption–desorption) process, and the magnitude of the effects of this process may be discussed in comparison with the standards.

Tailing solutes

Figs. 4–6 show various profiles of the tail production phenomenon observed for LSC of a polar solute at high solute dilution. The solute examined is trianisoyl-deoxycytidine, an intermediate product in chemical oligonucleotide synthesis[6]. We have studied the behaviour of these deoxynucleotide derivatives in LSC as examples of polar multi-functional solutes having various polar groups[3,4]. The present sample was chosen for its ease of detection within the linear isotherm range. This compound has been found to give asymmetric elution profiles under most LSC conditions, and the degree of peak asymmetry is higher than that of the corresponding less-polar tribenzoyl derivative.

A series of solvent mixtures, consisting of non-polar and polar solvents, are suitable for eluting a wide range of polar solutes from a silica gel column. For eluting highly polar solutes, such as nucleoside derivatives, and for dissolving water in the mobile phase without emulsification, the kinds of organic solvents available as polar components are limited (aliphatic alcohols, dioxane, etc.). Here, we used *n*-hexane–2-propanol mixtures in various proportions to examine a wide range of water concentrations. When these mixtures are used without adding water, the peaks of the solute examined become highly dispersed. It is very difficult to obtain clear chromatograms for such dispersing solutes at small sample sizes. Reliable curve fitting cannot be carried out without clear chromatograms. For this reason, comparisons were made by varying the amount of water added to the solvent mixtures.

Fig. 4 demonstrates the tail-reducing ability of water added to the mobile phase. Here, the horizontal coordinates are time relative to Gaussian retention time to compare tail lengths visually, because the retentivity changes greatly on increasing the water concentration from 0.1 to 0.3%. It can be clearly seen that the apparent tail area and length are greatly reduced as the water content increases.

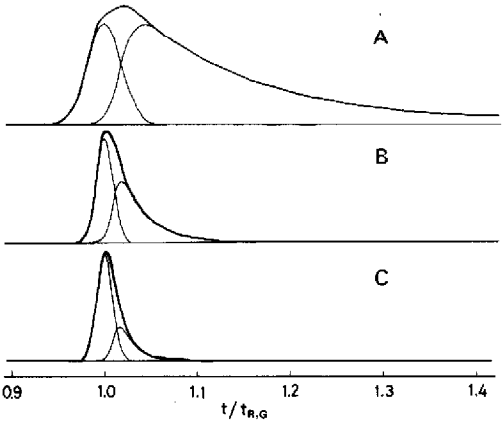

Fig. 4. Best fits of Chesler–Cram curves to experimental peaks of N,3′,5′-O-trianisoyldeoxycytidine, chromatographed on a silica gel column at a flow-rate of 1 ml/min with *n*-hexane–2-propanol–water mobile phases: (A) 70:30:0.1; (B) 70:30:0.3; (C) 70:30:0.5 (v/v).

Fig. 4A shows a peak obtained with the least amount of water (*ca.* 0.1%, v/v). This peak is highly asymmetric and its top shape differs greatly from the Gaussian shape. As discussed above, the Gaussian portion separated from such a peak is not likely to represent the distribution of solute molecules not captured by slow processes. The actual uncaptured molecule distribution may possibly have a much smaller population than that shown in Fig. 4A, as inferred from the top shape deviation from the Gaussian form.

As the water content increases to 0.3% or more, the peak tops become nearly symmetric and Gaussian (Fig. 4B and C). The uncaptured molecule distributions for these peaks may be accurately separated by the present curve-fitting procedure. The effects of water are thus analysed from Fig. 4B and C, although decreases in tail area and length are apparent when the water content increases from 0.1 to 0.3%. Both peaks have tails larger and longer than that of the standard peak (Fig. 3A), while the relative Gaussian widths ($\sigma_G/t_{R,G}$) are almost similar to the standard, as in Table II. This suggests that some kind of microscopic process that produce tails is operative in the LSC column, and variations in the degree of dispersion of elution peaks in LSC are almost solely due to this tail-producing process.

A slight increase in water content in the mobile phase from 0.3 to 0.5% leads to a *ca.* 26% decrease in tail length and a 45% decrease in tail area, the relative Gaussian width remaining almost constant. Such water effects are also evident in Fig. 5, where the 2-propanol concentration in the mobile phase is decreased to *ca.* 20% and the corresponding chromatogram at a 0.1% water content is replaced with that of a 0.2% content for the sake of analysis. In this instance, the fractional areas and relative lengths of tails are less than those in Fig. 4 at each water content, while the tendency for a decrease with increasing water content remains unchanged. The fractional tail area at a 0.5% water content (Fig. 5C) is comparable to that of the standard.

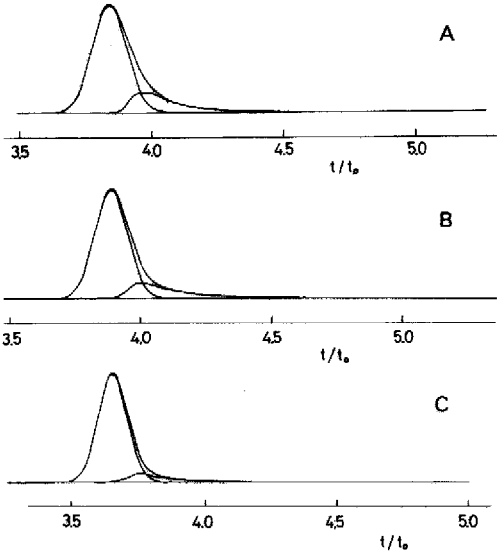

Fig. 6. Best fits of Chesler–Cram curves to experimental peaks of N,3′,5′-O-trianisoyldeoxycytidine, chromatographed on a silica gel column at a flow-rate of 4 ml/min with the same mobile phases as in Fig. 5.

slowly to form most of the apparent tail portion. As the flow-rate increases and the Gaussian retention time ($t_{R,G}$) is reduced, the number of captured solute molecules and the fractional tail area decrease, and the apparent tail length, determined by the rate constant of slow desorption, is magnified relative to $t_{R,G}$.

Here, it is expected that, if the tail-producing sites have higher adsorption rate constants for particular types of solutes, the fractional tail areas of the solutes will be larger at each flow-rate, and the degree of change in the fractional area observed with a flow-rate change will also be larger within the range of relatively small tail areas (<0.5 for the fractional area). This may actually be the case with the polar tailing solute, studied in this work, when compared with the less-tailing standard solute, where the difference in fractional tail area between the two experiments at different flow-rates is about six times larger for the former solute (at 0.2% water) than for the latter. The specificity of the tail-producing process for polar solutes is thus explained in terms of high adsorption rate constants for polar solutes at tail-

TABLE III

PEAK-SHAPE DATA OF N,3′,5′-O-TRIANISOYLDEOXYCYTIDINE, CHROMATOGRAPHED ON A SILICA GEL COLUMN AT A FLOW-RATE OF 4 ml/min

Mobile phase composition: n-hexane–2-propanol–water (v/v)	$a_T/(a_G + a_T)$	h_T/h_G	$10^3\sigma'_T/t_{R,G}$	$10^3\sigma_G/t_{R,G}$
80:20:0.2	0.199	0.182	22.2	16.3
80:20:0.3	0.174	0.140	22.9	15.2
80:20:0.5	0.097	0.073	21.3	14.5

producing sites and low desorption rate constants obviously observable as long apparent tails.

Based on the above interpretation, the effect of water added to the mobile phase is related to the kinetics of the tail-producing process. The fractional tail area is reduced with increasing water content at any flow-rate. The change in fractional tail area observed with flow-rate changes is also reduced with increasing water content. These effects indicate that the increase in water concentration leads to a decrease in the solute adsorption rate constant at tail-producing sites (and the number of captures of solute molecules per unit time period).

The effects of water on relative tail length is more difficult to explain. At a lower flow-rate, the relative tail length decreases with increasing water content, as observed above. More precisely, the relative tail height (h_T/h_G) decreases with increasing water to a lesser extent than that calculated from corresponding decrease in tail area (a_T/a_G), suggesting a reduction in dispersion of the captured solute molecules. This reduction can be caused by accelerating desorption from tail-producing sites. However, assuming the apparent tail to be composite and formed by two or more types of independent slow adsorption sites differing in kinetics, an alternative explanation may be suggested for this effect. If the tail-producing sites of the lowest desorption rate constant are chiefly responsible for the last-eluted part of the apparent tail portion and the adsorption on these sites is most specifically retarded by water, the fractional area of this part of the apparent tail may be most specifically reduced, leading to the tail height behaviour described here.

At higher flow-rates, the changes in relative tail length observed with increasing water content are less or not significant. That is, tail-height changes are nearly proportional to the corresponding changes in a_T/a_G and hence any significant reductions in tail dispersion (and acceleration of desorption) are not evident with increasing water content. This behaviour is explained without conflicting with that for the lower flow-rate, if we further assume variations in operative sites with changing flow-rate. If the more slowly desorbing sites have a less significant area in the apparent tail at this higher flow-rate because of their lower adsorption rates, the tail becomes no longer composite, and this behaviour is expected. Hence all changes in the relative tail length can be explained from the effect of water on the adsorption rate constant on tail-producing sites. In conclusion, water added to the mobile phase is likely to reduce tail dispersion by retarding the solute adsorption specifically for tail-producing sites from which solute molecules are more slowly desorbed, rather than by accelerating the desorption.

Role of mobile phase solvents

The role of mobile-phase solvents in determining the kinetics of tail-producing processes may be explained on the basis of the assumption of competitive adsorption at tail-producing active sites on silica surface. It is expected from the above discussion that, at tail-producing sites, adsorption rate constants may be higher and desorption rate constants lower for more polar solvents as well as for more polar solutes. The mobile phase is dynamically equilibrated with the stationary phase before solute samples are injected, and all stationary-phase adsorption sites are occupied by solvent molecules. The equilibrium constants for the adsorption of a component of the mobile phase on each type of adsorption site is given by the ratio of the rate constants

of adsorption and desorption of the component on the site from and into the solution. This ratio may be expected to be higher for more polar solvents and hence water, the most polar solvent used, may have the highest equilibrium constants for adsorption on tail-producing sites. As a result of the addition of water to the mobile phase system examined in this study, tail-producing sites may be extensively occupied by molecules of water even though its concentration in the mobile phase is low relative to the concentrations of the other components.

Polar molecules, adsorbed on the tail-producing sites, are likely to cause the kinetics of solute adsorption to be so slow as to produce tails, as the molecular exchange rate on surface sites is decreased by adsorption of polar solvents. In particular, water molecules may retard the adsorption kinetics to such an extent that solute adsorption virtually, does not occur. Hence water molecules may reduce the number of available tail-producing sites by preferential adsorption and, therefore, decrease the (apparent) adsorption rate constant.

As in Figs. 5 and 6, $t_{R,G}$ does not decrease greatly with increasing water content beyond 0.2%, and a slight increase in $t_{R,G}$ is observed with a water content increase from 0.2 to 0.3%. Such effects were also found for other solutes in similar systems[3,11] and considered to be related to the virtual completion of a water monolayer on the silica surface and with a decrease in the solute activity coefficient in the stationary phase due to the hydration of solute molecules, adsorbed on the water layer, with excessive water molecules in the stationary phase[12]. The results of this study suggest that, at a water concentration in the range 0.2–0.5%, a very small number of the surface-active sites that are not occupied by water molecules have virtually no influence on retention time, but are still operative for the tail production.

As the concentration of 2-propanol in the mobile phase increases from 20 to 30%, while the water content remains constant at 0.3 or 0.5%, the equilibrium concentration of water in the stationary phase decreases owing to the competitive effect of 2-propanol and/or to a decrease in the activity coefficient of water in the mobile phase. This may result in an increase in the number of available tail-producing sites and, therefore, an increase in the solute adsorption rate constant and tail area, as is evident in Table II.

However, it can be expected that if the water content is increased simultaneously with 2-propanol, additional water may counterbalance the effect of 2-propanol, supplementing the number of adsorbed water molecules for tail-producing sites. This is also evident in Table II. At a 0.3% water concentration, the fractional tail area increases by a factor of *ca.* 1.8 with an increase in 2-propanol concentration from 20 to 30%. When the water concentration is increased from 0.3 to 0.5% with this 2-propanol increase, no significant change is observed in fractional tail area (Table II). Hence experimental data support the explanation of the role of polar molecules in influencing solute adsorption kinetics on tail-producing sites.

Dependence of tail production on solute residence time in the mobile and stationary phases

Here, we return to the tail area changes observed with flow-rate changes. Considering the roles of adsorbed solvent molecules influencing tail areas, it might be possible that these changes include those resulting from a change in the equilibrium composition of the stationary phase, which is induced by a pressure change incidental

to a flow-rate change. This was checked by experiment. The change in pressure equivalent to that due to a flow-rate increase was attained by connecting packed columns to the outlet of the detector, but any significant changes could not be observed in the fractional tail area with this pressure change. The stationary phase composition may not vary significantly in the range of flow-rates studied. Therefore, we can conclude that these tail-area changes represent purely the dependence of tail production on the residence time of the solute zone in the column and that the fractional tail area is actually an increasing function of this time.

The solute residence time in the column is divided by time in the mobile phase (hold-up time, t_0) and in the stationary phase (net retention time). We have explained the effects of 2-propanol on apparent tails regardless of those on solute retention time. However, if the mechanism of the tail-producing process involves, as its first step, ordinary rapid adsorption, which, by itself, determines the retention time of the Gaussian zone, the fractional tail area must depend on the net retention time for the Gaussian component ($t_{R,G} - t_0$). Such a secondary adsorption was found in reversed-phase liquid chromatography for various proteins as a result of their conformational unfolding in the alkyl-bonded stationary phase[13]. In this instance, the degree of unfolding and secondary adsorption, observed as the appearance of an extra later eluting peak, was a function of the time the solute is in contact with the bonded-phase surface (the net retention time of the original peak).

If the tail-producing processes are not such secondary transitions of the adsorbed state of solute molecules and occur independently, the fractional tail area should not be dependent on the net retention time but be merely a function of the hold-up time. This appears actually to be the case in the LSC tail-producing process when the effects of 2-propanol on solute retention have no relation to tail area. Tail production persists when polar solutes are eluted with a time almost equal to the hold-up time (with almost zero net retention time). The tail-producing process is hence due to slow adsorption–desorption processes occurring independently of the rapid solute exchange that determines Gaussian retention.

CONCLUSIONS

The results of this study demonstrate that the problem of peak tailing in LSC at high solute dilution may be treated as a kinetic effect of distinctively slow adsorption–desorption processes in column development. The appearance of peak tails depends on the mobile-phase flow-rate and the polarity of the solute and solvent. Although the tail-producing process is analogous to a rapid adsorption–desorption process with respect to solute specificity (or selectivity), the tail production may be caused by the presence of a small number of surface-active sites which have virtually no influence on solute retention. For suppressing the tail production, a slightly excess amount of water should be added to the mobile phase compared with the minimum amount of water required to eliminate the effect of surface-active sites on solute retention.

From a practical point of view, we suggest the use of a mixture of a polar organic solvent and a small amount of water, which, as a set of polar components with a fixed mixing ratio, may be diluted with a non-polar solvent to construct an LSC mobile-phase system. This mobile-phase system may be useful for maintaining

the effective amount of adsorbed water for tail reduction over a wide range of polar organic component concentrations and, therefore, for attaining almost Gaussian elution profiles for a wide range of polar solutes. It will therefore enhance the chromatographic resolution of complex mixture samples.

REFERENCES

1 J. C. Giddings, *Dynamics of Chromatography, Part I, Principles and Theory*, Marcel Dekker, New York, 1965.
2 J. C. Giddings, *Anal. Chem.*, 35 (1963) 1999.
3 S. Hara and T. Ohkuma, *J. Chromatogr.*, 316 (1984) 389.
4 T. Ohkuma and S. Hara, *J. Chromatogr.*, 323 (1985) 227.
5 S. N. Chesler and S. P. Cram, *Anal. Chem.*, 45 (1973) 1354.
6 H. Schaller, G. Wiedemann, B. Lerch and H. G. Khorana, *J. Am. Chem. Soc.*, 85 (1963) 3821.
7 S. M. Roberts, D. H. Wilkinson and L. R. Walker, *Anal. Chem.*, 42 (1970) 886.
8 J. R. Conder, *J. High Resolut. Chromatogr. Chromatogr. Commun.*, 5 (1982) 341.
9 J. P. Foley and J. G. Dorsey, *J. Chromatogr. Sci.*, 22 (1984) 40.
10 L. R. Snyder and J. J. Kirkland, *Introduction to Modern Liquid Chromatography*, Wiley, New York, 1979.
11 J. E. Paanakker, J. C. Kraak and H. Poppe, *J. Chromatogr.*, 149 (1978) 111.
12 A. Rizzi, *J. Chromatogr.*, 348 (1985) 1.
13 K. Benedek, S. Dong and B. L. Karger, *J. Chromatogr.*, 317 (1984) 227.